DUNE potential for sub-GeV dark matter in proton beam dump mode

Sabeeha Naaz, Jyotsna Singh and R. B. Singh

Abstract :

In this work we have explored the DUNE (Deep Underground Neutrino Experiment) potential for capturing the sub-GeV dark matter in viable dark matter parameter space. For this we have used DUNE near detector whose sensitivity for the detection of the signatures of dark matter candidate depends on beam energy; size, geometry and material of the detector; angle acceptance of detector and mitigation of neutrino background. To consider the dark matter candidates in physics framework the standard model is extended by introducing an extra dark gauge group $U(1)_D$ which couples to the standard model hypercharge $U(1)_Y$ gauge group via vector portal by using kinetic mixing term ε. As dark matter produced here uses 120 GeV proton beam facility of DUNE therefore three channels π^0/η-decay, proton bremsstrahlung and parton-level are used for dark matter production which are relevant in this energy range. The neutrino background is minimized by using DUNE experiment in beam dump mode. To explore the new region of parameter space of dark matter at DUNE near detector the elastic scattering of dark matter beam with electrons and nucleons are studied. The simulation result shows that DUNE can capture dark matter signatures for larger parameter space of $(m_\chi, \varepsilon^2\alpha_D)$ in comparison to the other existing dark matter probes for example BaBar, E137, LSND, MiniBooNE, T2K etc.

Keywords: Dark matter, dark photon, direct detection, beam dump, yield, sensitivity.

1 Introduction:

The existence of dark matter is strongly suggested by various gravitational phenomenon in astrophysics and cosmology [1]. The simplest realization of dark matter particles is in form of new stable weakly interacting non-baryonic elementary particles, which can be relativistic or non-relativistic. The presence of such particles have motivated experimentalist to design experiments capable of capturing dark matter (DM) signals. The three main experimental techniques which are used to probe the dark matter particles are (i) Indirect Detection experiments [2, 3, 4] (ii) Direct Detection experiments [5] and (iii) Collider searches [6, 7, 8, 9]. In direct detection mode the dark matter particles collide with the standard model particles and the study of recoil nucleons or scattered electrons provide the information regarding dark matter candidates. While the observation of standard model (SM) particles created during the annihilation or decay of dark matter particles will come under indirect detection searches. Further in collider searches dark matter beam is produced by the collision of highly energetic particles. The mass of different DM candidates, which are postulated using different inputs of physics varies from 10^{-31} to 10^{20} GeV. The present research on the DM candidates can be divided on the basis of detection techniques, type of its interaction and DM masses i.e. axion DM produced from the non-thermal mechanism $\mathcal{O}(eV)$, light or sub-GeV DM $\mathcal{O}(MeV - GeV)$ and weakly interacting massive particles (WIMPs) $(> 1GeV)$ are produced from the thermal freeze-out mechanism. Due to absence of the signatures of DM candidates the cosmologist have speculated different types of the DM, whose classification depends on the kinetic energy possessed by the DM. If the DM particles are relativistic or super-relativistic they are called hot DM [10] otherwise they are called cold DM. Since the hot dark matter particle are moving with relativistic or super-relativistic speed hence they will escape from small density fluctuations. If the DM particles are moving very fast then the structure formation theory predicts that all structures smaller than massive galaxies would be destroyed by free streaming process while their exist structures smaller than galaxies therefore we can assume that DM can not be predominantly hot. In this way we can assume that a little bit of hot DM is mixed with predominant cold DM.

Sabeeha Naaz, Dr. Jyotsna Singh and Dr. R. B. Singh
University of Lucknow, Department of Physics,Lucknow-226007,India e-mail: sabeehanaaz0786@gmail.com e-mail: singh.jyotsnalu@gmail.com e-mail: rajendrasinghrb@gmail.com

In one of the strongly motivated idea, DM particles are considered as the natural partners of the existing standard model particles and originate from the unification frameworks or axions invoked to solve the strong CP violation problems. The line of thought followed for the production of DM particles will determine the method or the experimental techniques, required for the detection of DM. The sensitivity of these experiments must allow the experimental facility to explore new interaction channels, whose cross-sections are below the cross-section of electroweak interaction of the SM particles. With these types of experiments we can try to achieve the required relic DM density without depending on either weak scale mass or weak scale interaction. Thermal relic dark matter are the particles which were created thermally in the early universe, when the temperature of the universe was sufficiently high and thermal equilibrium for DM particle was achieved (i.e. annihilation and creation rates of DM was roughly equal), making dark matter density constant. As the universe was cooling and expanding the DM density began to fall down because the DM creation stopped due to cooling but annihilation of the DM continued, till the time the temperature of the universe was higher than the mass of DM. When the temperature dropped below the mass of the DM, the annihilation process of DM also stopped making the DM density constant (freeze-out) at this temperature.

The cosmological abundance of thermal relic DM can provide the measure of annihilation rate of DM $\langle \sigma v \rangle$ [11]. The annihilation rate of DM can be expressed as,

$$\langle \sigma v \rangle = x + yv^2 + ... \tag{1}$$

First term of above equation indicates the annihilation cross-section arising from the s-wave which is independent of the relative velocity of DM (v) whereas the second term gives the contribution arising from partial p-wave which depends on the square of relative velocity of DM. The s-wave contribution dominates in the thermally averaged annihilation cross-section ($\langle \sigma v \rangle_s \approx 2.2 \times 10^{-26} cm^3 s^{-1}$) but adding p-wave contribution to it gives precise value of relic DM density. In our model we have considered s-wave and p-wave contributions since the detection of annihilation cross-section arising from partial waves other than s-wave will provide a crucial clue regarding the nature of DM. However these detection become inefficient for heavy DM (WIMP) candidates.

The null results estimated by the direct detection technique [12, 13, 14, 15, 16] used for the capturing of DM signatures of mass range 1 GeV to 1 TeV has ruled out the large region of DM parameter space. These results motivate us to move towards the the discovery of production modes, which can produce lower mass DM candidates (below 1 GeV). This selection was inspired by the observation of 511 keV γ -ray line arising from the galactic center with the help of SPI (SPectrometer INTEGRAL) spectrometer [17, 18]. It was also inspired by many theoretical models i.e. supersymmetric (SUSY) model of DM, in this supersymmetric model SUSY partner particle for each SM particle is included and by adding these particles the supersymmetric models attempt to address problems, which are beyond the purview of SM. The SUSY model for DM predicts the precise annihilation cross-section of DM which can generate the correct thermal relic DM abundance [19, 20, 21]. One more relevant theoretical approach to detect sub-GeV DM is asymmetry DM (ADM) model. This ADM model relates the asymmetry of dark matter to the asymmetry of baryon. In the present universe, DM density is approximately five times of the SM baryon density [22]. If the production channel for the creation of the dark matter density and baryonic density in the early universe is assumed to be the same then DM relic density can be naturally explained with the help of ADM model framework [23, 24, 25, 26].

The characteristics of weak-scale (low mass mediator) parameter offers a hope for direct detection of non-gravitational DM interactions in laboratory. However these searches are less sensitive to light DM candidates due to the low detection threshold of recoil nucleon, thus it is essential to consider alternative approach to detect light DM in this regime (sub-GeV range). Keeping all of the above points in our mind new strategy is introduced to provide required valuable sensitivity to sub-GeV DM in fixed target experiments. One major issue with fixed target experiments is the presence of high neutrino background which make it difficult to discriminate between the signatures of DM particles and neutrino present in the background. The use of experiment in beam dump mode reduces the neutrino background in the target volume. This beam dump facility was used by the MiniBooNE experiment [31] for the detection of DM.

DUNE with its cutting edge technology is designed to study the neutrino science and proton decay physics. This facility can be further exploited for the study of the ground breaking discoveries i.e. origin of matter, unification of forces, dark matter detection etc. Therefore in this paper, we have investigated the sensitivity of DUNE near detector [32] for light dark matter in beam dump mode. High intensity proton beam of 120 GeV produced at Fermi lab main injector of DUNE experiment is made to collide with fixed target.

On collision it produces neutral and charged mesons these neutral mesons further decay into a DM beam and charged mesons are dumped in a pipe before they can decay into neutrino backgrounds. Because of highly energetic proton beam of DUNE experiment DM particles are produced via three different channels: mesons decay, bremsstrahlung and parton-level production channel. The physics used here for the study of DM candidates, considers the interaction of hidden sector (Hypercharge field strength $F^{Y}_{D\mu\nu}$) with standard model (SM) particles (Hypercharge field strength $F^{Y}_{\mu\nu}$) via vector portal. For DM detection we have used direct detection technique. By using this technique we impose constraints on the mass of DM such that the DM mass lies well below the Lee-Weinberg bound [29] to get the correct relic abundance [30]. The signatures of these DM particles are identified by two different scattering modes i.e. its scattering with the nucleons and electrons presence in the downstream near detector. To check the sensitivity of DUNE near detector for sub-GeV DM we have used BdNMC simulation tool [33].

This paper is organized as follows. In section 2, we have described the physics model of light DM, different modes of DM production, scattering signatures of DM candidates at DUNE near detector and we have also defined several experimental and theoretical constraints which are relevant for sub-GeV DM. In section 3, we have briefly discussed BdNMC simulation tool. DUNE DM sensitivity results are discussed in section 4. The work is summarized in section 5 with concluding remarks.

2 Formalism:

2.1 Dark Matter Portals

In an attempt to understand the universe, theoretical physicists have used different portals [27] which establish a connection between the hidden sector and visible sector. Portals acts like a bridge between dark matter and ordinary matter and they exchange specific mediator between them. The hidden sector mediators can be scalar, pseudoscalar, vector or fermionic. The Lagrangian of different dominant portals with associated mediators are as follows [28]:

$$\mathcal{L}_{portal} = \begin{cases} -\varepsilon F_{\mu\nu} F_D^{\mu\nu} & \text{Vector Portal :: Vector} \\ (\mu S + \lambda S^2) H H^{\dagger} & \text{Higgs Portal :: Scalar} \\ y_{ij} L_i H N_j & \text{Neutrino Portal :: Fermion} \\ \frac{a}{f_a} A_{\mu\nu} \tilde{A}^{\mu\nu} & \text{Axion Portal :: Pseudoscalar} \end{cases} \tag{2}$$

Here, ε is the kinetic mixing term, $F_{\mu\nu} = [\partial_\mu F_\nu - \partial_\nu F_\mu]$ is the SM hypercharge field strength tensor, $F_{D_{\mu\nu}} = [\partial_\mu \gamma_{D_\nu} - \partial_\nu \gamma_{D_\mu}]$ is field strength of dark sector $U(1)_D$, H is the SM Higgs doublet, S is a scalar singlet of new dark sector $U(1)_D$, λ and μ are free parameters, L is a lepton doublet, i and j are flavor indices, N_j is right handed state for Majorana mass term, f_a is mass scale of pseudoscalar a and $A_{\mu\nu}(\tilde{A}^{\mu\nu})$ is the (dual) field strength tensor of the SM photon field.

We have focused on the vector portal which is the most viable portal for the production of light dark matter because the "kinetic mixing" interaction term "$\varepsilon F_{\mu\nu} F_D^{\mu\nu}$" is invariant under gauge transformation of both $U(1)_D$ and $U(1)_Y$ in this scenario. To consider the DM candidates the SM can be extended by adding a new extra dark gauge group $U(1)_D$ that couples to the SM hypercharge $U(1)$ gauge group via kinetic mixing term ε [34, 35]. The dark gauge group $U(1)_D$ symmetry is spontaneously broken at a low energy scale by the Higgs in hidden sector and leads a massive dark photon (DP) mediator γ_D which is a hypothetical particle of $U(1)_D$ gauge group. Experimental searches of dark photon is needs of great interest for DM physics community and these searches are carried out at LHC and other experiments. Here we have focused on the MeV to GeV mass range of dark photons because this mass scale of dark photon will be able to describe the results of astrophysical evidences regarding DM density. The DM particle χ can be taken as scalar or fermionic fields which are charged under dark gauge group $U(1)_D$. We have focused on scalar field of DM candidates because this scenario is less constrained by astrophysical considerations, such as annihilation-induced distortion of the CMB.

The applicable low energy Lagrangian of light scalar dark matter for vector portal can be expressed as,

$$\mathcal{L}_{DM} = \mathcal{L}_{\gamma_D} + \mathcal{L}_{\chi} \tag{3}$$

where,

$$\mathcal{L}_{\gamma_D} = -\frac{1}{4}F_{D_{\mu\nu}}F_D^{\mu\nu} + \frac{1}{2}m_{\gamma_D}^2\gamma_{D_\mu}\gamma_D^\mu - \frac{1}{2}\varepsilon F_{D_{\mu\nu}}F^{\mu\nu} \tag{4}$$

$$\mathcal{L}_\chi = \frac{ig_D}{2}\gamma_D^\mu J_\mu^\chi + \frac{1}{2}\partial_\mu\chi^\dagger\partial_\mu\chi - m_\chi^2\chi^\dagger\chi \tag{5}$$

where, $J_\mu^\chi = [(\partial_\mu\chi^\dagger)\chi - \chi^\dagger(\partial_\mu\chi)]$ is DM current density and g_D is treated as gauge coupling constant between DM current density and a new massive dark photon field potential γ_D^μ originated from spontaneously broken gauge symmetry $U(1)_D$. At low energies, DP kinetically mixes with ordinary photon and couples to the SM electromagnetic current with strength εg, where g is electromagnetic coupling constant.

This minimal light dark matter model consist of four parameters, dark matter mass (m_χ), dark photon mass (m_{γ_D}), gauge coupling (g_D) and kinetic mixing term (ε). The viable sub-GeV scale DM under the Lee-Weinberg bound provides a fix relation among all parameters and can give correct relic DM density [36].

The sub-GeV thermal relic DM candidates are constrained by annihilation cross-section $\langle\sigma v\rangle \sim 1pb$ in which thermal relic DM abundance are compatible with the observed relic DM density. Many experimental constraints are present for the selection of parameter space of light DM i.e. strongest constraints on DM-electron scattering are imposed by LSND experiment [49, 51, 40, 64], CRESST-II [62] direct detection search places constraints on the large value of fine structure parameter (α_D) of hidden sector, BaBar [37] experiment is mono-photon searches provides constraint on the mass of DM is $m_\chi > 60MeV$, beam dump experiment E137 [65] is sensitive for light DM with 20 GeV electron beam and NA64 collaboration [38] recently provides a strong constraints on the mass of dark photon which should be below 100 MeV.

The reachable parameter space by neutrino facilities is $m_{\gamma_D} > 2m_\chi$ and $g_D \gg \varepsilon g$ which suggests that dark photon mostly decays into dark matter pair and for this situation the annihilation cross-section of scalar DM into leptons is given by [39]:

$$\sigma(\chi\chi^\dagger \to l\bar{l})v \sim \frac{8\pi v^2 Y}{m_\chi^2} \tag{6}$$

where,

$$Y = \varepsilon^2\alpha_D\left(\frac{m_\chi}{m_{\gamma_D}}\right)^4; \alpha_D = \frac{g_D^2}{4\pi} \tag{7}$$

and v is relative velocity of DM. Since the DM annihilation cross-section depends on Y therefore we have explored the correlation between (Y, m_χ) and $(\varepsilon, m_{\gamma_D})$ for DUNE detector.

2.2 Production of the Dark Matter Candidates

Several models have been developed to study the light DM candidates. Amongst these models we have to select one, which contains in itself a viable annihilation channels to be studied at the selected experiment. We have selected a dark matter physics model which works for light DM candidates and can be used for DM beam produced at fixed target neutrino experiments. Near detector of a fixed target neutrino experiments are designed to detect the neutrino signatures but here we want to check their sensitivity for DM detection [40]. The idea behind the DM detection by the fixed target neutrino experiments is as follows: a highly intense proton beam interacts with the fixed target and produces dark photons which further decays into DM candidates. In this way beside neutrino beam, a DM beam is also produced in neutrino experiments. In the presence of neutrino beam the detection of DM particles will be difficult as the neutrino beam will act as a background and this background will add huge errors in the detection of DM. Therefore beam dump mode is selected for exploring the sensitivity of DUNE. In this mode proton beam interacts with the beryllium target and produces charged pions which are aligned using magnetic horns towards a steel absorber (beam dump) where these pions decay into neutrinos. In this way nearly pure DM beam is produced in beam dump mode.

Here most of the light dark photons are produced from the decay of neutral mesons. Some heavy dark photons are also produced from the resonance vector mesons and from the hadron-level interactions. Keeping in mind that beam energy of DUNE flux is high here we summarize the three production modes of light dark matter.

1. π^0/η mesons decay: relevant for lower masses of dark photon.
2. Resonant vector mesons (Bremsstrahlung) decay: relevant for intermediate masses of dark photon.
3. Direct or parton-level production from quarks and gluon constituents: relevant for higher masses of dark photon (m_{γ_D}>1 GeV).

2.2.1 π^0/η mesons decay in flight:

At lower energies the neutral mesons decay channel dominates over other channels for the over all production of dark photon. These mesons are produced from the primary interaction of $p(p)$ and $p(n)$.

$$p + p(n) \rightarrow X + \pi^0, \eta \rightarrow X + \gamma + \gamma_D \rightarrow X + \gamma + \chi + \chi^\dagger \tag{8}$$

This DM production process depends on the beam energy and configuration of target because decay of mesons can happen either inside the target or in successive decay volume. Since the mesons distribution varies with the beam energy hence different experiment needs different analytical fit $f(\theta, p)$ for mesons distribution in θ and p plane, to generate the distribution of DM flux. For proton beam energy considered in this work (120 GeV for DUNE) the analytical distribution for mesons considered is BMPT (Beryllium Material Proton Target) distribution [41]. Using this distribution in appropriate energy range of mesons we get $\sigma_{pp\rightarrow pp\pi^0} \approx 27\sigma_{pp\rightarrow pp\eta}$ [42].

If the mass of neutral meson is greater than the mass of the dark photon i.e. $m_{\gamma_D} < m_\delta$ $(\delta = \pi^0, \eta)$ or if the mass of DM particle produced is such that $2m_\chi < m_{\gamma_D} < m_\delta$ then γ_D will be produced on-shell and it will decay into DM candidates. Branching ratio of mesons decay to dark matter using narrow width approximation [43] is equal to the product of mesons decay to dark photons and dark photon to dark matter. The production of dark photon depends on ε^2 and ratio of m_{γ_D} and m_δ while it is independent of m_χ and α_D.

$$Br(\delta \rightarrow \gamma\chi\chi^\dagger) = Br(\delta \rightarrow \gamma\gamma_D)Br(\gamma_D \rightarrow \chi\chi^\dagger) \tag{9}$$

$$Br(\delta \rightarrow \gamma\gamma_D) \simeq 2\varepsilon^2 \left(1 - \frac{m_{\gamma_D}^2}{m_\delta^2}\right)^3 Br(\delta \rightarrow \gamma\gamma) \tag{10}$$

Where $Br(\pi^0 \rightarrow \gamma\gamma) \simeq 1$ and $Br(\eta \rightarrow \gamma\gamma) \simeq 0.39$. For completeness, the dark photon always decay into DM indicates; $Br(\gamma_D \rightarrow \chi\chi^\dagger) \simeq 1$, which requires $\varepsilon \ll 1$ condition.

For off-shell production of dark photon i.e. $2m_\chi > m_{\gamma_D}$ or $m_{\gamma_D}^2 \gtrsim m_\delta^2 - 2\Gamma_{\gamma_D} m_{\gamma_D}$ (where Γ_{γ_D} is decay width of DP), the narrow width approximation is not a viable choice. This production mode does not have any analytical form like in the case of on-shell production. Here the DM production is calculated by by three body decay and branching ratio, branching ratio for off-shell dark matter production is expressed as [44],

$$Br(\delta \rightarrow \gamma\chi\chi^\dagger) = \frac{\varepsilon^2\alpha_D}{\Gamma_\delta} \times \frac{1}{4\pi m_\delta} \int d\Psi_{\delta\rightarrow\gamma\gamma_D} d\Psi_{\gamma_D\rightarrow\chi\chi^\dagger} dq_{\gamma_D}^2 |A_{\delta\rightarrow\gamma\chi\chi^\dagger}|^2 \tag{11}$$

where $d\Psi$ is two body phase-space, $q_{\gamma_D}^2$ is momentum of DP, Γ_δ is total decay width of π^0 and η, and $A_{\delta\rightarrow\gamma\chi\chi^\dagger}$ is three body decay normalized amplitude.

$$|A_{\delta\rightarrow\gamma\chi\chi^\dagger}|^2 = \frac{\varepsilon^2\alpha_D\alpha^2}{\pi f_\delta^2[(q_{\gamma_D}^2 - m_{\gamma_D}^2)^2 + m_{\gamma_D}^2\Gamma_{\gamma_D}^2]}[(q_{\gamma_D}^2 - 4m_\chi^2)(m_\delta^2 - q_{\gamma_D}^2)^2 - 4q_{\gamma_D}^2(p.k_1 - p.k_2)^2] \tag{12}$$

Where, f_δ is meson (π^0, η) decay constant, p and q_{γ_D} are momenta of ordinary photon and dark photon respectively, k_1 and k_2 are momenta of dark matter and anti dark matter produced in the final state.

The total dark matter particles produced via both on-shell and off-shell production can be written as,

$$N_\chi = \sum_{on-shell+off-shell} Br(\delta \rightarrow \gamma\chi\chi^\dagger) \times \delta\_per\_\pi^0 \times \pi^0\_per\_POT \times POT \tag{13}$$

where, $\delta\_per\_\pi^0 = 1$ for π^0 and $\delta\_per\_\pi^0 = 0.11$ for η which gives the π^0 production 27 times that of η production. $\pi^0\_per\_POT$ and which is number of π^0 per proton on target (POT) is equal to 4.5 [45] for DUNE.

2.2.2 Resonant vector mesons (proton Bremsstrahlung) decay:

Proton bremsstrahlung production process becomes effective for intermediate mass range of mediators. The dark photon produced in this process is via the scattering of proton by nucleons of fixed target which is similar to the ordinary proton bremsstrahlung.

$$p + p(n) \rightarrow p + p(n) + \gamma_D,$$

In this process a nearly collimated beam of dark photon is generated. The four momentum assigned to incident proton of mass m_p is $q = (E_p, 0, 0, Q)$ where $E_p = Q + \frac{m_p^2}{2Q}$. The four momentum of outgoing dark photon of mass m_{γ_D} is $q_{\gamma_D} = (E_{\gamma_D}, q_\perp \cos(\phi), q_\perp \sin(\phi), Q.z)$ where $E_{\gamma_D} = Q.z + \frac{q_\perp^2 + m_{\gamma_D}^2}{2Q.z}$, $Q.z = q_\parallel$ and z is a fraction of proton beam momentum carried away by outgoing DP in the direction of proton beam. Here $q_\perp$ and $q_\parallel$ are transverse and longitudinal components of γ_D momenta.
By Weizsäcker-Williams approximation the rate of dark photon production per proton is as follows [46, 47],

$$\frac{d^2 N_{\gamma_D}}{dz dq_\perp^2} = \frac{\sigma_{pA}(2m_p(E_p - E_{\gamma_D}))}{\sigma_{pA}(2m_p E_p)} F_{1,N}^2(q^2) f_{yx}(z, q_\perp^2) \tag{14}$$

here $\sigma_{pA} = f(A)\sigma_{pp}$, $f(A)$ is a function of atomic number A and $f_{yx}(z, q_\perp^2)$ is a splitting weight-function of photon which relates before and after scattering differential cross section [46],

$$f_{yx}(z, q_\perp^2) = \frac{\varepsilon^2 \alpha}{2\pi H}\left[\frac{1+(1-z)^2}{z} - 2z(1-z)\left(\frac{2m_p^2 + m_{\gamma_D}^2}{H} - z^2\frac{2m_p^4}{H^2}\right) + 2z(1-z)(z+(1-z)^2)\frac{m_p^2 m_{\gamma_D}^2}{H^2} + 2z(1-z)^2\frac{m_{\gamma_D}^4}{H^2}\right]$$

here $H = q_\perp^2 + (1-z)m_{\gamma_D}^2 + z^2 m_p^2$ and α is electromagnetic fine structure constant.

Since radiative γ_D has time-like momentum and time-like form factor $F_{1,N}(q^2)$ expresses off-shell mixing with vector mesons in appropriate kinematic region. Vector portal consider only proton form factor $F_{1,p}(q^2)$ [48] which incorporates both ρ-like (isovector) and ω-like (isoscalar) Breit-Wigner components [48] and this form factor is not completely resolved for ρ and ω. Above 1 GeV, the form factor suppresses the rate of production of virtual photons and at this moment direct parton level production comes into play.

To calculate the dark photon production rate, equation [14] must be integrated over $p_\perp$ and z for a range that satisfies some kinematic conditions [46]:

$$E_p, E_{\gamma_D}, E_P - E_{\gamma_D} \gg m_p, m_{\gamma_D}, |q_\perp| \tag{15}$$

We have selected a range $z \in [0.2, 0.8]$ and $|p_\perp| = 0.4$ for DUNE which satisfied the above conditions.

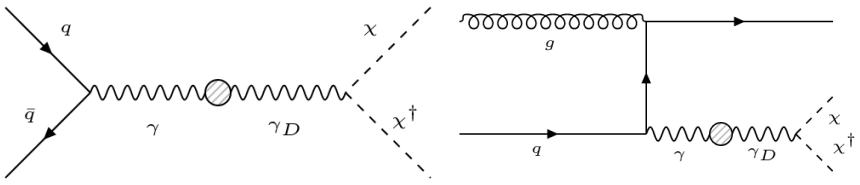

Fig. 1: Parton-level production of scalar dark matter via vector portal.

2.2.3 Direct production of dark matter from Drell-Yan process:

Parton-level production mechanism is very interesting as it provides a portal for the production of high energetic dark photon. Direct production of dark photons from Drell-Yan process is shown in figure [1].

$$p + p(n) \to X + \gamma_D \to X + \chi\chi^\dagger \tag{16}$$

This process will use the narrow width approximation for on-shell DM production [49] and this approximation is valid up to the second order. The dark matter production cross-section as a function of lab frame DM energy E_χ and angle between the direction of proton beam and lab frame momentum of DM ϕ can be expressed as,

$$\frac{d^2\sigma(p+p(n)\to X+\gamma_D\to X+\chi\chi^\dagger)}{dE_\chi d\cos\phi} = \left[\frac{\partial(x,\cos\hat{\phi})}{\partial(E_\chi,\cos\phi)}\right] \times \frac{d\sigma(pp(n)\to\gamma_D)}{dz} Br(\gamma_D\to\chi\chi^\dagger) g(\cos\hat{\phi}) \tag{17}$$

where $\hat{\phi}$ is angle between momentum of dark matter candidate and proton beam, in the dark photon rest frame, and square bracket term is a Jacobian function. The g function gives the angular distribution of the dark matter in γ_D rest frame for scalar DM produced via a vector mediator and it can be expressed as,

$$g(\cos\hat{\phi}) = \frac{3}{4}(1-\cos^2\hat{\phi}) \tag{18}$$

the direct production cross-section of dark photon is [49],

$$\sigma(pp(n)\to\gamma_D) = \int_\zeta^1 \frac{d\sigma(pp(n)\to\gamma_D)}{dx}dx = \frac{4\pi^2\alpha\varepsilon^2}{m_{\gamma_D}^2}\sum_q Q_q^2 \int_\zeta^1 \frac{dx}{x}\tau\left[f_{q/p}(x)f_{\bar{q}/p(n)}(\frac{\zeta}{x}) + f_{\bar{q}/p}(x)f_{q/p(n)}(\frac{\zeta}{x})\right] \tag{19}$$

where Q_q is quark charge in the unit of positron electric charge, $\zeta = m_{\gamma_D}^2/s$ and $\sqrt{s}$ is the hadron-level center of mass energy. $f_{q/p(n)}(x)$ is the parton distribution function (PDF) which gives the probability of extraction of quarks and gluons from proton(neutron) with longitudinal momentum fraction x. To evaluate cross-section, we have used CTEQ6.6 PDFs [50] and have set $Q = m_{\gamma_D}$ which is varied in range of $m_{\gamma_D}/2$ to $2m_{\gamma_D}$.
To produce the dark matter we integrate the equation [17] over the DM lab frame energy and angle between proton beam direction and momentum of DM lab frame.

2.3 Scattering and Cross-Section of Dark Matter Beam:

In this work we explore the allowed parameter space for capturing dark matter signatures at DUNE experiment through elastic neutral current-like (NCE-like) scattering of DM candidate with nucleons and electrons.

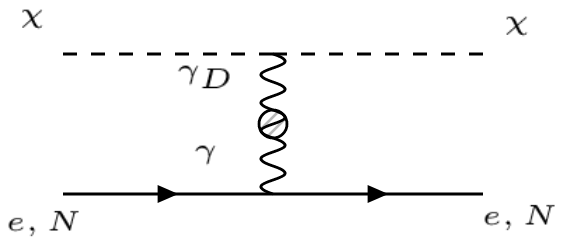

Fig. 2: Tree-level DM scattering with nucleons and electrons via vector portal.

2.3.1 Elastic neutral current-like scattering with electrons:

The differential cross-section of DM elastic scattering with electrons [51] as a function of scattered electron energy (E_e) is given below:

$$\frac{d\sigma_{\chi e\to\chi e}}{dE_e} = 4\pi\alpha\alpha_D\varepsilon^2 \times \frac{2m_eE^2 - (2m_eE + m_\chi^2)(E_e - m_e)}{(E^2 - m_\chi^2)(m_{\gamma_D}^2 + 2m_eE_e - 2m_e^2)^2} \tag{20}$$

where m_e is mass of the electron, m_χ is mass of the dark matter and E is the energy of incoming dark matter.

2.3.2 Elastic neutral current-like scattering with nucleons:

Scattering of scalar DM with nucleons via vector mediator is similar to the neutrino-nucleon scattering via Z-mediator [52]. The differential cross-section of incoherent elastic scattering of dark matter with free nucleons with respect to the outgoing dark matter energy (E_χ) can be expressed as [51, 53],

$$\frac{d\sigma_{\chi N\to\chi N}}{dE_\chi} = 4\pi\alpha\alpha_D\varepsilon^2 \times \frac{F_{1,N}^2(Q^2)A(E,E_\chi) - \frac{1}{4}F_{2,N}^2(Q^2)B(E,E_\chi)}{(m_{\gamma_D}^2 + 2m_N(E - E_\chi))^2(E^2 - m_\chi^2)} \tag{21}$$

where E and E_χ represents energy of incoming and outgoing dark matter and $Q^2 = 2m_N(E - E_\chi)$ is the transferred four momentum. Function A and B are expressed as:

$$A(E,E_\chi) = 2m_NEE_\chi - m_\chi^2(E - E_\chi) \tag{22}$$

$$B(E,E_\chi) = (E_\chi - E)[(E_\chi + E)^2 + 2m_N(E_\chi - E) - 4m_\chi^2] \tag{23}$$

The contribution to this cross-section arises from both nucleons: protons and neutrons hence their form factors are present in the above equation [21]. $F_{1,N}$ and $F_{2,N}$ represent monopole and dipole form factors of nucleons respectively and can be expressed as,

$$F_{1,N} = \frac{q_N}{(1 + Q^2/m_N^2)^2}; F_{2,N} = \frac{\kappa_N}{(1 + Q^2/m_N^2)^2} \tag{24}$$

where q_p = 1, q_n = 0, κ_p = 1.79, and κ_n = -1.9, all values are in units of nuclear magnetons. Above scattering equation stands only for free nucleons but we know that in a nucleus bound nucleons also exist. Therefore we can use effective differential cross-section with a consideration of bound nucleons. The effective differential cross-section can be written as,

$$\frac{d\sigma_{\chi N\to\chi N}^{eff}}{dE_\chi} = \left[\frac{1}{7}C_{pf}(Q^2) + \frac{3}{7}C_{pb}(Q^2)\right]\frac{d\sigma_{\chi p\to\chi p}}{dE_\chi} + \frac{3}{7}C_{nb}(Q^2)\frac{d\sigma_{\chi n\to\chi n}}{dE_\chi} \tag{25}$$

where C's are the relative efficiencies of dark matter scattering with free proton (C_{pf}), bound proton (C_{pb}), bound neutron (C_{nb}) and they are the function of momentum transfer Q^2.

2.4 Constraints on Minimal Light Dark Matter Model:

In our work we have considered the coupling of hidden sector with SM particles via vector portal. A benchmark model of light DM is required to describe the coupling of hidden sector with SM. To make the considered model viable with the detection technologies several constraints needs to be imposed on the parameters of the model, which are summarized below in brief.

- ***Thermal relic DM constraints:*** The constraints imposed by WMAP (Wilkinson Microwave Anisotropy Probe) on the thermal relic DM density, $\Omega_{DM}h^2 \sim 0.1 \sim (0.1pb)/\langle\sigma v\rangle_{fo}$ ($h = 0.710 \pm 0.025$ is Hubble constant in the unit of 100 km $sec^{-1}Mpc^{-1}$) introduces the DM annihilation cross-section at freeze-out

to be $\langle\sigma v\rangle_{fo} \sim 1pb$. Generally, if DM annihilation cross-section is $\langle\sigma v\rangle_{fo} \gtrsim 1pb$ then it does not provide enough contribution to the relic DM abundance.

- ***CMB and BBN constraints on light DM:*** The constraints on DM annihilation cross-section are introduced by the CMB too. The cross-section considered should be such that they do not distort the CMB due to energy injection. The constraint imposed by WMAP7 on the DM annihilation cross-section is $f(z)\langle\sigma v\rangle_{CMB} \lesssim 0.1(m_\chi/GeV)pb$, here $f(z)$ is an efficiency factor which depends on the redshift z. For the lower masses of DM, efficiency factor f varies from $f \sim 0.2$ for pion in the final state to $f \sim 1$ for electron in the final state [56][49]. These constraints excludes the thermal relic DM abundance below the few GeV DM masses via s-channel annihilation. The DM annihilation cross-section via is s-wave (thermally averaged annihilation cross-section is independent of time) suppressed and therefore have less impact on BBN (Big Bang Nucleosynthesis) [57].
- ***Bullet cluster and cluster lensing constraints:*** The constraint on DM self scattering cross-section imposed by bullet cluster and cluster lensing observations [58][59] is given by,

$$\frac{\sigma}{m_\chi} \lesssim few \times \frac{cm^2}{g} \tag{26}$$

As it is obvious from equation [6] and equation [7] that above defined constraint will impose bound on the fine structure constant α_D of the hidden sector at lower DM masses [39].

$$\alpha_D \lesssim 0.06 \times \sqrt{\left(\frac{MeV}{m_\chi}\right)} \times \left(\frac{m_{\gamma_D}}{10MeV}\right)^2 \tag{27}$$

In our work we have used the benchmark value of $\alpha_D = 0.5$.

- ***Constraints on the kinetic mixing term ε:*** Kinetic mixing parameter ε defines the kinetic mixing of dark photon of hidden sector with ordinary photon of SM via vector portal. Recent bound on ε are set by invisible decay [60, 74] and supernovae [61]. The invisible decay of J/ψ (e.g. $J/\psi \to \gamma_D^* \to \chi\chi^\dagger$) and $\Upsilon(1S)$ decay (e.g. $\Upsilon(1S) \to \gamma_D^* \to \chi\chi^\dagger$) imposes constraints on the upper limit, $\alpha_D\varepsilon^2 \lesssim few \times 10^{-4}$ for lower DM masses. While the lower limit is imposed by the observation of supernovae which is $\alpha_D\varepsilon^2 \gtrsim few \times 10^{-14}$.
- ***Direct detection constraints:*** The recent constraints to the direct detection of light DM are imposed by CRESST-II [62] and CDMS-Lite [63]. The CRESST-II experiment can explore the sensitivity of DM masses below 0.5 GeV with detection threshold of nuclear recoil 307 eV. Whereas CDMS-lite experiment can detect the electron recoils as low as 56 eV for DM masses $\mathcal{O}$(MeV-GeV) hence DM-electron scattering can reach towards lower masses of DM.
- ***Beam dump experiment constraints:*** LSND fixed target proton beam dump experiment provides a way to investigate sub-GeV DM. This experiment suggests the strongest bounds for on-shell DM production mode $m_{\gamma_D} \lesssim m_{\pi^0}$ via $p + p(n) \to X + \pi^0 \to X + \gamma + \gamma_D \to X + \gamma + \chi + \chi^\dagger$ [49, 51, 40, 64], these DM candidates when scattered through electrons and nucleons looks similar to neutrino neutral-current scattering signature. The E137 fixed target electron beam dump experiment [65] is sensitive for $e + p(n) \to e + p(n) + \gamma_D \to e + p(n) + \chi + \chi^\dagger$ in a downstream detector. The DM production yield depends on Y, "Y" is expressed as $Y = \varepsilon^2\alpha_D\left(\frac{m_\chi}{m_{\gamma_D}}\right)^4$, scales with $\varepsilon^2\alpha_D$ and the ratio of m_χ and m_{γ_D}. The ratio, $m_\chi/m_{\gamma_D} = 1/3$ is most conservative value for the estimation of the DM yield, the larger value of ratio will call stronger constraints for the estimation of the DM yield.
- ***BaBar experiment:*** A mono-photon search performed at BaBar experiment [37] imposes constraint on the mass of dark photon which further invisibly decays into DM. This experiment eliminates the existence of dark photon with the limits m_{γ_D}<8 GeV and $\varepsilon > 10^{-3}$ for $m_\chi > 60$ MeV.
- $K^+ \to \pi^+\nu\bar{\nu}$***:*** The result of E949 experiment at Brookhaven National Laboratory places a limit on kinetic mixing parameter $\varepsilon^2 > 3 \times 10^{-5}$ for MeV-GeV mass scale of dark photon [66, 67].
- ***Electron/Muon*** $g-2$***:*** The blue band shown in the figure [4] [5] [6] and [7] is the region where the consistency of theoretical and experimental value improves to with in 3σ. Leaving this space all other parameter space is excluded as it increases the disagreement of either muon or electron $g-2$ to more than 5σ [68, 69, 70].

3 Simulation Technique:

We have used BdNMC (Beam dump Neutrino Monte Carlo) [33] simulation tool to find out the sensitivity of DUNE for DM detection. The DM beam is generated via three different modes; (i) Mesons decay: essential parameters for meson decay channel considered in our work are $\delta\_per\_\pi^0 = 1$ for π^0, $\delta\_per\_\pi^0 = 0.11$ for η and $\pi^0\_per\_POT = 4.5$ [45]. (ii) Bremsstrahlung decay: in proton bremsstrahlung mode DM beam is produced through the decay of ρ and ω resonant vector mesons. (iii) parton-level: for parton-level process we have used CTEQ6.6 parton distribution function to generate DM beam. The details of DM beam production is mentioned in section(3). The BMPT distribution function is used to produce DM beam through above three modes. A highly intense proton beam interacts with beryllium target in the fixed target DUNE experiment and produces DM particles via all relevant channels. These DM particles propagate through decay volume and reach the DUNE near detector. A brief description of DUNE parameters considered in our work are listed below [54]:

Name	Target material	E_{beam}	POT	Detector mass (Fiducial)	Distance	Angle	Efficiency(ε_{eff})
DUNE	$Ar+CH_4$	120 GeV	1.1×10^{21}	1 ton(900 Kg + 100 Kg)	574 m	0	0.9 [55]

Table 1: Essential parameters for DUNE near detector.

Cuts on the recoil energy of nucleons	Cuts on the recoil energy of electrons	Forward angle cuts on electrons
$E_R \in [0.1, 2]$ GeV	$E_e \in [0.1, 2]$ GeV	$\theta_e \in [0.01, 0.02]$

Table 2: Energy and angle thresholds for the electrons and nucleons of considered DUNE near detector.

Elastic scattering of DM candidates by electron and nucleons are studied in our work. The expression for the combination of total DM signal events observed is taken as [33],

$$N_{\chi A\to\chi A} = N_A \varepsilon_{eff} \sum_{p.c.} \left(\frac{N_\chi}{2N_{trials}} \sum_i L_i \sigma_{\chi A,i} \right) \tag{28}$$

where ε_{eff} is the detection efficiency of detector, $N_{A(e,p,n)}$ is the electron and nucleon density of target atoms in the detector and p.c. mentions the relevant production channel of DM. The N_{trials} is number of trajectories generated by the Monte Carlo. The inner summation is over 4-momenta of dark matter produced by the Monte Carlo and L_i is the length of the intersection between dark matter trajectory (4-momentum) and the detector. The DM total cross-section $\sigma_{\chi A}(E)$ is taken as [33],

$$\sigma_{\chi A}(E) = \int_{E_\chi^{min}}^{E_\chi^{max}} dE_\chi \sum_{A=e,p,n} f_A \frac{d\sigma_{\chi,A}}{dE_\chi} \tag{29}$$

where E is the energy of incoming dark matter, E_χ is the energy of outgoing dark matter and $E_\chi^{min/max}$ is minimum and maximum outgoing DM energy which is calculated by the experimental cuts on the electron/nucleon recoil momentum q, which can be expressed as $\sqrt{2M(E-E_\chi)}$. For vector portal in elastic or quasi-elastic scattering we take $f_{p,n,e}$ = Z, A - Z, Z.

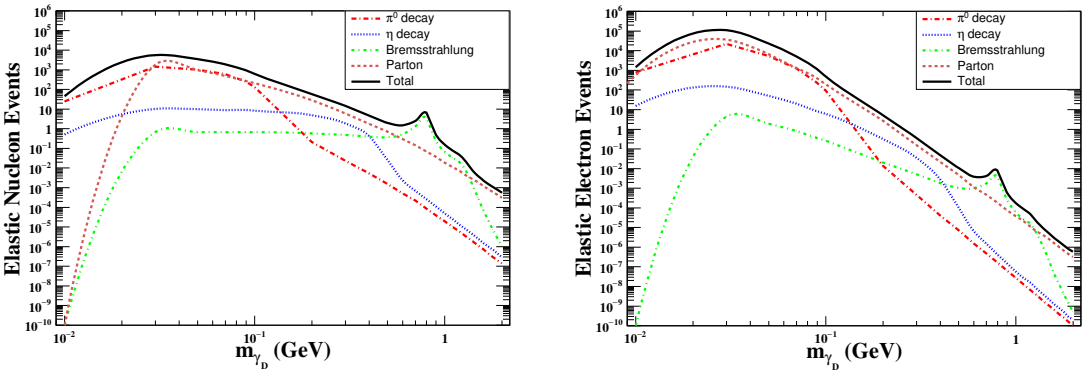

Fig. 3: The event rate of DM elastic scattering with nucleons (left panel) and electrons (right panel) versus dark photon mass from distinct channels by using 120 GeV beam energy. Here we have considered m_χ = 0.01 GeV, $\varepsilon = 10^{-3}$ and $\alpha_D = 0.5$.

3.1 Viability of the model:

We have focused on the sub-GeV mass range of DM candidates in the proton fixed target experiment to probe the thermal relic DM by considering a model in which a massive dark photon mediator γ_D, a hypothetical particle belonging to $U(1)_D$ gauge group kinetically mixes with the ordinary photon of the SM through the kinetic mixing term ε. To address the discrepancy observed between the experimental and theoretical values of the anomalous magnetic moment $(g-2)$ of leptons, the model under consideration keeps the window open (with DUNE) for handling the $(g-2)$ anomaly. The mono-photon searches at Belle-II [75] experiment will further decide the viability of the vector portal. The collider searches for missing energy and momentum can further add information to the dark matter model. The forthcoming e-ASTROGAM [76] a gamma ray telescope will offer important platform to discover dark matter particles with masses below $\sim$ 10 MeV and check the viability of the model. Further CRESST-II experiment pushes down the mass of DM below 1 GeV in the direct detection technique. In this way we can see that the fusion of all approaches will allow us to pin down the dark matter parameter space.

4 Results and Discussion:

We have simulated, the production of DM by using 120 GeV proton beam in beam dump mode. Taking proton beam energy into consideration the DM candidate are produced, using three different modes (i) mesons decay [13] (ii) bremsstrahlung process [14] (iii) parton level production [19]. The elastic scattering of DM with electrons [20] and nucleons [21] of near detector is studied to check the sensitivity of DUNE for the DM parameter space $(\varepsilon, m_{\gamma_D})$ and (Y, m_{γ_D}). The near detector parameters used for this analysis are defined in table [1] and [2].

In figure [3] we have plotted the DM scattering events as a function of dark photon mass (m_{γ_D}). The DP mass range considered by MiniBooNE [33] for similar analysis is from 0.01 to 1 GeV whereas we have considered the mass range of DP from 0.01 to 2 GeV in this analysis as the proton beam used is more energetic. The entire DP mass range is divided into three regions for analysis study of DM:

1. $m_{\gamma_D} \leq 0.1$ GeV
2. $0.1 \leq m_{\gamma_D} \leq 1.0$ GeV
3. $m_{\gamma_D} \geq 1.0$ GeV

In the first region of DP mass, the contribution to DM events arising from mesons decay and parton level production is approximately $\sim$ 38.5% and $\sim$ 61.4% respectively, while bremsstrahlung process contributes negligibly. As we move towards the second region of DP , the contribution to the DM events arising from parton level production increases from $\sim$ 61.4% to $\sim$ 84% (roughly) and the contribution from

bremsstrahlung process also increases and becomes $\sim 10\%$ while DM production from mesons decay becomes negligible. To mention, a sharp peak in bremsstrahlung DM events is observed at ~ 800 MeV which can be attributed to the resonance production of m_ρ and (m_ω). In the third region of DP mass, almost all the contribution of DM production comes from parton level production channel. The above analysis depends on the energy of the proton beam as well as detector technology. As it is evident from figure [3] the DM-nucleon scattering events (left panel) will provide an effective way for the detection of DM candidates in the higher mass range of DP ($m_{\gamma_D} \gtrsim 100$ MeV) while DM-electron scattering events (right panel) will provide a promising way for the observance of DM candidates for lower masses of dark photon. In this observation the value of kinetic mixing term ε is kept constant at $\varepsilon = 10^{-3}$.

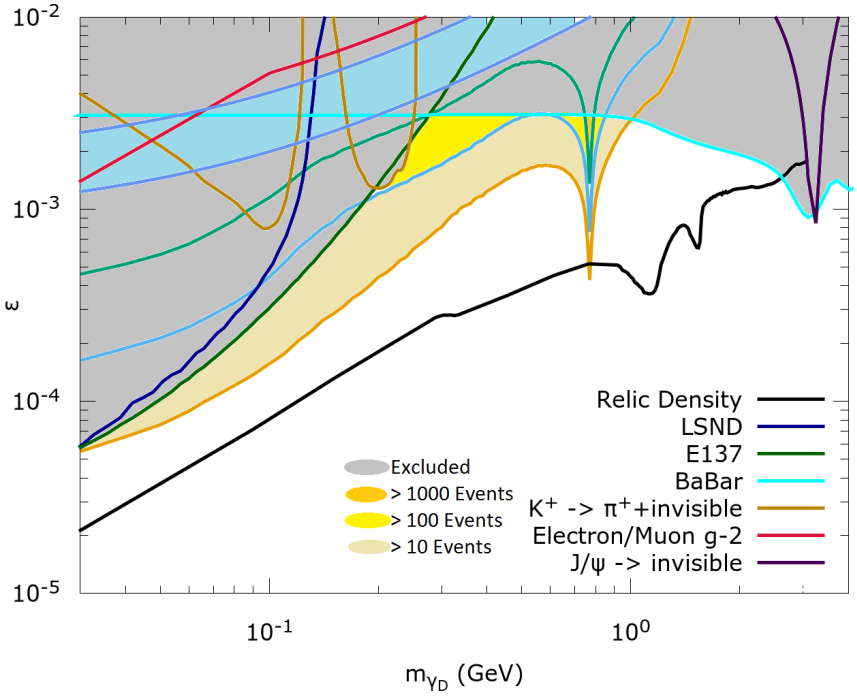

Fig. 4: The contour sensitivity plot for light dark matter signatures (elastically scattered with nucleons) at DUNE in the parameter space of $(\varepsilon, m_{\gamma_D})$. These dark matter are produced from distinct channels by using 120 GeV proton beam. Here we have considered $m_\chi = 0.01$ GeV, $\alpha_D = 0.5$ and POT = 1.1×10^{21}. In above plot, the gray regions are excluded by existing constraints, while the yellow contours indicate 10, 100 and 1000 events and black line shows thermal relic dark matter (freeze-out).

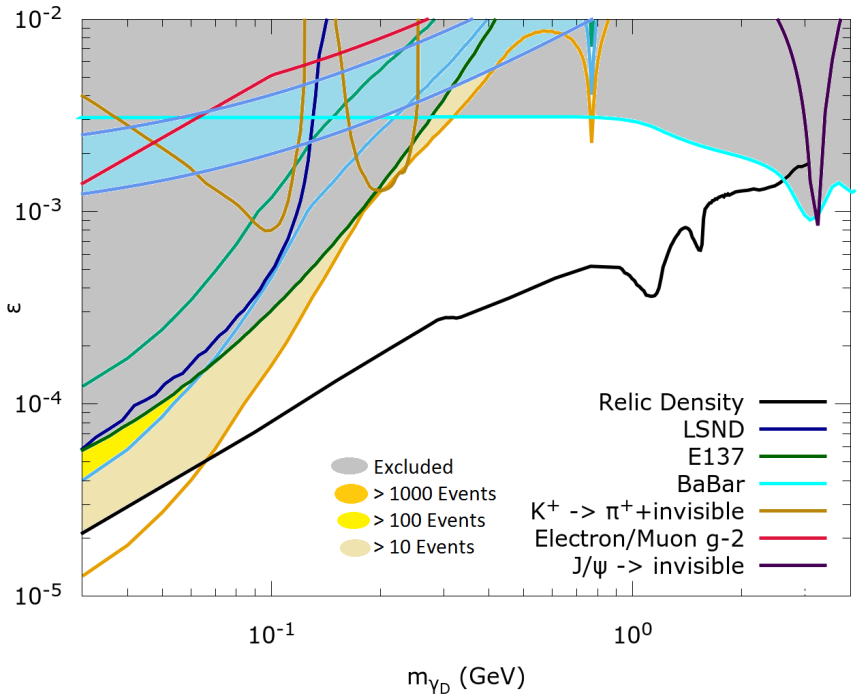

Fig. 5: The contour sensitivity plot for light dark matter signatures (elastically scattered with electrons) at DUNE in the parameter space of $(\varepsilon, m_{\gamma_D})$. These dark matter are produced from distinct channels by using 120 GeV proton beam. Here we have considered $m_\chi = 0.01$ GeV, $\alpha_D = 0.5$ and POT = 1.1×10^{21}. In above plot, the gray regions are excluded by existing constraints, while the yellow contours indicate 10, 100 and 1000 events and black line shows thermal relic dark matter (freeze-out).

To better constrain the DM parameter space, the DM parameter ε is allowed to vary between 10^{-2} to 10^{-5} and DP mass is allowed to vary in the range from 0.03 GeV to 2 GeV for the fixed mass of DM (0.01 GeV). Figures [4] and [5] shows the allowed region of DM parameter space $(\varepsilon, m_{\gamma_D})$ for DUNE experiment after several important constraints are applied to that parameter space. A realistic constraint applied from thermal relic abundance of DM is shown by black line in the above figures. The threshold values for recoil nucleons (figure [4]) and scattered electrons (figure [5]) are mentioned in table[2]. The three sensitivity contours for 10, 100 and 1000 events of DUNE are plotted using elastic scattering of DM with nucleons and electrons for a given mass of DM (10 MeV) in parameter space $(\varepsilon, m_{\gamma_D})$. From our analysis we can observe that the DM-electron scattering is more sensitive to lower kinetic mixing term and lower mass parameter space $(\varepsilon, m_{\gamma_D})$. Whereas A sharp increase in DUNE sensitivity is observed at ~ 800 MeV mass of m_{γ_D} which can be attributed to the resonance production at $m_{\gamma_D} \sim m_\rho(m_\omega)$ via bremsstrahlung. In figures [4] and [5], we have shown several experimental and theoretical constraints by different colors as mentioned in legends and excluded region is shown by gray color. From figure [4] we have observed that the allowed parameter space between two sensitivity contours 10 and 100 events is $[m_{\gamma_D} \in (0.03, 1) GeV, \varepsilon \in (6 \times 10^{-5}, 3 \times 10^{-3})]$. While the allowed parameter space between two sensitivity contours 100 and 1000 events is $[m_{\gamma_D} \in (0.2, 1) GeV$, $\varepsilon \in (7 \times 10^{-4}, 3 \times 10^{-3})]$. Similarly in figure [5], the allowed parameter space between two sensitivity contours 10 and 100 events is $[m_{\gamma_D} \in (0.03, 0.4) GeV, \varepsilon \in (2 \times 10^{-5}, 4 \times 10^{-3})]$ whereas parameter space between two sensitivity contours 100 and 1000 events is $[m_{\gamma_D} \in (0.03, 0.06) GeV, \varepsilon \in (4 \times 10^{-5}, 2 \times 10^{-4})]$. Figures [4] and [5] shows that like DUNE, the LSND and E137 experiments are also sensitivity for lower value of ε but their sensitivity for higher DP is far below than DUNE.

In the figure [6] and [7] DM mass (m_χ) have been varied from 10 MeV to 1000 MeV and kinetic mixing parameter (ε) have been varied from 10^{-5} to 10^{-1}. A fixed number of DM scattering events are selected to illustrate the DUNE sensitivity for sub-GeV DM. For the generation of these DM scattering events,

$m_{\gamma_D} = 3m_\chi$ and fine structure constant of hidden sector $\alpha_D = 0.5$ are taken into consideration. Since a given mass of dark matter produced by dark photon are of different energies hence no linear trend between m_χ and ε are observed. The threshold values for recoil nucleons (figure [6]) and scattered electrons (figure [7]) are mentioned in table[2]. The parameter space (Y, m_χ) is shown in figure [6] and [7] for different number of events i.e. 10, 100 and 1000 events. A sharp increase in DUNE sensitivity is observed at ~ 300 MeV mass of m_χ which can be attributed to the resonance production at $m_\chi = \frac{m_{\gamma_D}}{3} \sim \frac{m_\rho(m_\omega)}{3}$ via bremsstrahlung. Different experimental and theoretical constraints are shown in figures [6] and [7] which gives allowed regions for dark matter parameter space. From figure [6] we have observed that the favorable region of parameter space between two sensitivity contours 10 and 100 events is $[m_\chi \in (0.01, 0.3)GeV,\ Y \in (2\times10^{-11}, 3\times10^{-8})]$, the favorable region of parameter space between two sensitivity contours 100 and 1000 events is $[m_\chi \in (0.05, 0.3)GeV,\ Y \in (2\times10^{-10}, 3\times10^{-8})]$ and the allowed region of parameter space above the contour of 1000 events is $[m_\chi \in (0.07, 0.3)GeV,\ Y \in (2\times10^{-9}, 3\times10^{-8})]$. Similarly in figure [7], the favorable region of parameter space between two sensitivity contours 10 and 100 events is $[m_\chi \in (0.01, 0.1)GeV,\ Y \in (2\times10^{-12}, 3\times10^{-8})]$ and the favorable region of parameter space between two sensitivity contours 100 and 1000 events is $[m_\chi \in (0.01, 0.03)GeV,\ Y \in (1\times10^{-11}, 1\times10^{-10})]$. Figures [6] and [7] shows that like DUNE, the LSND and E137 experiments are also sensitivity for lower value of ε but their sensitivity for higher DP is far below than DUNE whereas Direct detection detection experiment is sensitive till 1 GeV mass of DM for higher values of kinetic mixing parameter.

From above analysis we have concluded that DM-nucleon scattering events allow larger parameter space for a large DM mass range whereas DM-electron scattering events shows good sensitivity for lower region of parameter space.

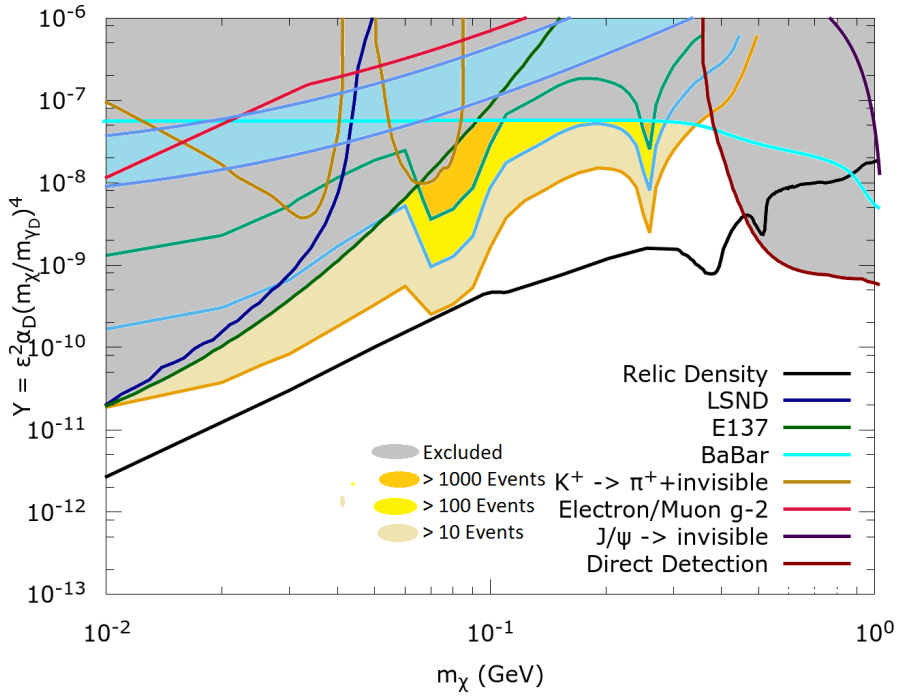

Fig. 6: The contour sensitivity plot for light dark matter signatures (elastically scattered with nucleons) at DUNE in the parameter space of (Y, m_χ). These dark matter are produced from distinct channels by using 120 GeV proton beam. Here we have considered $m_{\gamma_D} = 3m_\chi$, $\alpha_D = 0.5$ and POT = 1.1×10^{21}. In above plot, the gray regions are excluded by existing constraints, while the yellow contours indicate 10, 100 and 1000 events and black line shows thermal relic dark matter (freeze-out).

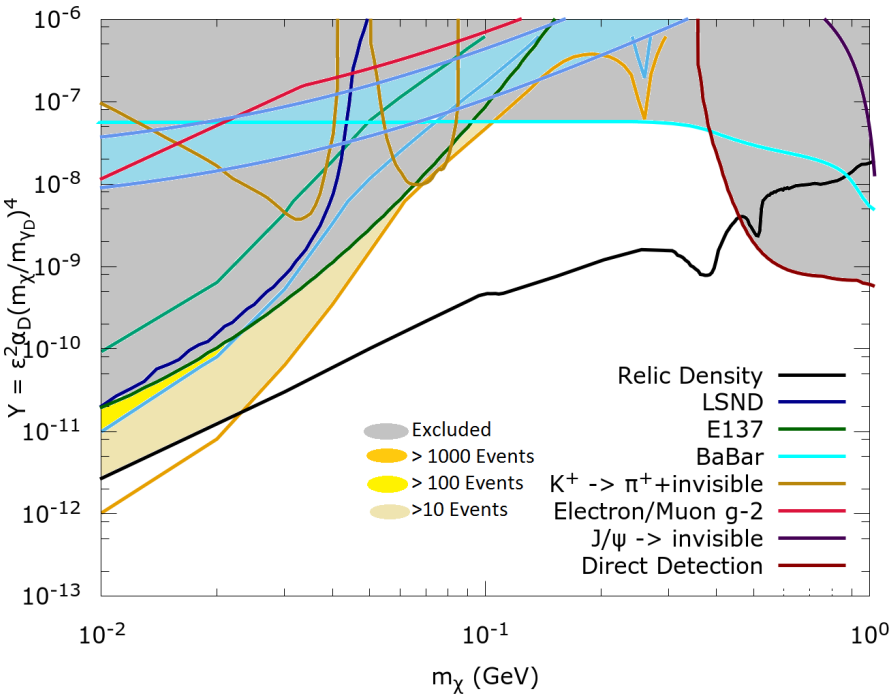

Fig. 7: The contour sensitivity plot for light dark matter signatures (elastically scattered with electrons) at DUNE in the parameter space of (Y, m_χ). These dark matter are produced from distinct channels by using 120 GeV proton beam. Here we have considered $m_{\gamma_D} = 3m_\chi$, $\alpha_D = 0.5$ and POT = 1.1×10^{21}. In above plot, the gray regions are excluded by existing constraints, while the yellow contours indicate 10, 100 and 1000 events and black line shows thermal relic dark matter (freeze-out).

5 Conclusion:

In this work we have explored the sensitivity of DUNE near detector for the detection of sub-GeV DM. The DM is accommodated by adding $U(1)_D$ gauge group to SM gauge group. In this model the dark photon of gauge group $U(1)_D$ kinetically mixes with the photon of $U(1)_Y$ gauge group via kinetic mixing parameter ε. The Lagrangian of our considered DM model for scalar DM is expressed in equation (3). The DM is produced via three production modes and then rate of DM scattering with electrons and nucleons is monitored. The simulated study of the sub-GeV DM production and detection at DUNE near detector through direct detection technique at fixed target, in beam dump mode is of great importance for particle physics. The dark matter parameter space are constrained by many experimental and theoretical constraints that are explained in the section (2.4).

This study throws light on hidden sector and the potential of DUNE for probing non standard physics by looking at the sub-GeV DM signatures via DM-nucleon and DM-electron scattering at DUNE near detector. The results indicates that the DM-electron scattering is more efficient at lower masses, whereas DM-nucleon scattering sensitivity is better in higher masses regime. The DUNE experiment will be sensitive to the larger parameter space of $(m_\chi, \varepsilon^2\alpha_D)$ in comparison to other proton beam fixed target experiments i.e. LSND and MiniBooNE [33, 73, 30, 74]. Present constrained on DM parameter space imposed by DUNE is better constrained by prospective constraints on DM parameter space by the different experiments. We have observed that the sensitivity of DUNE detector for sub-GeV DM is roughly 50% better as in comparison to neutrino experiments. As this study is performed in DM parameter space $(\varepsilon, m_{\gamma_D})$ and (Y, m_χ) by taking the thermal relic DM density (black line) for scalar DM candidates as benchmark. The fine structure constant

of hidden sector is $\alpha_D = 0.5$ in our analysis. In upcoming work we will try to explore the sensitivity plot for different values of α_D too.

Acknowledgements We would like to thank Raj Gandhi and Sajjad Athar for their valuable discussions.

References

1. Dark Matter Strategic Review 2020, Science and Technology Facilities Council, https://stfc.ukri.org/files/2019-dark-matter-strategic-review/.
2. Timothy Cohen et al., Wino Dark Matter Under Siege, (2013), arXiv:1307.4082v3 [hep-ph].
3. JiJi Fan and Matthew Reece, In Wino Veritas? Indirect Searches Shed Light on Neutralino Dark Matter, (2013), arXiv:1307.4400v1 [hep-ph].
4. A. Hryczuk et al., Indirect Detection Analysis: Wino Dark Matter Case Study, (2014), arXiv:1401.6212v2 [astro-ph.HE].
5. G. Angloher et al., Results from 730 kg days of the CRESST-II Dark Matter Search, (2012), arXiv:1109.0702v1 [astro-ph.CO].
6. B. Bhattacherjee et al., Phenomenology of Light Fermionic Asymmetric Dark Matter, (2013), arXiv:1306.5878v2 [hep-ph].
7. M. Blennow et al., Asymmetric Dark Matter and Dark Radiation, (2012), arXiv:1203.5803v2 [hep-ph].
8. D. E. Kaplan et al., Asymmetric Dark Matter, (2009), arXiv:0901.4117v1 [hep-ph].
9. Ian-Woo Kim and K. M. Zurek, Flavor and Collider Signatures of Asymmetric Dark Matter, (2013), arXiv:1310.2617v1 [hep-ph].
10. S. Profumo et al., An Introduction to Particle Dark Matter, (2019), arXiv:1910.05610v1 [hep-ph].
11. Anirban Das and Basudeb Dasgupta, Selection Rule for Enhanced Dark Matter Annihilation, (2017), arXiv:1611.04606v3 [hep-ph].
12. E. Aprile et al., (XENON100 Collaboration), Dark Matter Results from 225 Live Days of XENON100 Data, (2012), arXiv:1207.5988v2 [astro-ph.CO].
13. G. Angloher et al., Results on light dark matter particles with a low-threshold CRESST-II detector (CRESST Collaboration), Eur. Phys. J. C76 no. 1, (2016) 25, arXiv:1509.01515 [astro-ph.CO].
14. R. Agnese et al., (SuperCDMS Collaboration), WIMP-Search Results from the Second CDMSlite Run, (2016), arXiv:1509.02448v2 [astro-ph.CO].
15. A. Tan et al., (PandaX-II Collaboration), Dark Matter Results from First 98.7 Days of Data from the PandaX-II Experiment, (2016), arXiv:1607.07400v3 [hep-ex].
16. D. S. Akerib et al., Results from a search for dark matter in the complete LUX exposure, (2017), arXiv:1608.07648v3 [astro-ph.CO].
17. N. Prantzos et al., The 511 keV emission from positron annihilation in the Galaxy, (2010), arXiv:1009.4620v1 [astro-ph.HE].
18. L. Bouchet et al., On the morphology of the electron-positron annihilation emission as seen by SPI/INTEGRAL, (2010), arXiv:1007.4753v1 [astro-ph.HE].
19. D. Hooper and K. M. Zurek, Natural supersymmetric model with MeV dark matter, Phys.Rev.D77, 087302 (2008).
20. J. L. Feng and J. Kumar, The WIMPless Miracle: Dark Matter Particles without Weak-scale Masses or Weak Interactions, (2008), arXiv:0803.4196v3 [hep-ph].
21. J.L. Feng, H. Tu, and H.B. Yu, Thermal Relics in Hidden Sectors, (2008), arXiv:0808.2318v3 [hep-ph].
22. P. Ade et al., (Planck Collaboration), Planck 2013 results. I. Overview of products and scientific results , (2013), arXiv:1303.5062v2 [astro-ph.CO].
23. D. B. Kaplan, Single Explanation for Both Baryon and Dark Matter Densities, Phys. Rev. Lett.68, 741 (1992).
24. G. R. Farrar and G. Zaharijas, Dark Matter and the Baryon Asymmetry of the Universe, (2004), arXiv:hep-ph/0406281v3.
25. K. M. Zurek, Asymmetric Dark Matter: Theories, Signatures, and Constraints, (2013), arXiv:1308.0338v2 [hep-ph].
26. T. Cohen, D.J. Phalen, A. Pierce and K. M. Zurek, Asymmetric Dark Matter from a GeV Hidden Sector, (2010), arXiv:1005.1655v1 [hep-ph].
27. Sabeeha Naaz, Jyotsna Singh and R. B. Singh, DUNE prospect for leptophobic dark matter, (2020), arXiv:2004.10996 [hep-ph].
28. J. Alexander et al., Dark Sectors 2016 Workshop: Community Report, (2016), arXiv:1608.08632v1 [hep-ph].
29. B.W. Lee and S. Weinberg, Cosmological Lower Bound on Heavy-Neutrino Masses, Phys. Rev. Lett. 39 (1977) 165.
30. Valentina De Romeri, Kevin J. Kelly and Pedro A. N. Machado, DUNE-PRISM sensitivity to light dark matter, Phys. Rev., D 100, 095010 (2019).
31. R. Dharmapalan et al., (The MiniBooNE Collaboration), Low Mass WIMP Searches with a Neutrino Experiment:A Proposal for Further MiniBooNE Running, (2012), arXiv:1211.2258v1 [hep-ex].
32. R. Acciarri et al., (The DUNE Collaboration), Long-Baseline Neutrino Facility (LBNF) and Deep Underground Neutrino Experiment (DUNE), (2016), arXiv:1601.02984v1 [physics.ins-det].
33. Patrick deNiverville et al., Light dark matter in neutrino beams: production modelling and scattering signatures at MiniBooNE, T2K and SHiP, arXiv:1609.01770v3 [hep-ph].
34. B. Holdom, Two U(1)'s and Epsilon Charge Shifts, Phys. Lett. B166 (1986)196.
35. L. B. Okun, Limits on electrodynamics: paraphotons?, (1982), Zh. Eksp. Teor. Fiz. 83,892-898.
36. M. Pospelov, A. Ritz and M. B. Voloshin, Secluded WIMP Dark Matter, (2007), arXiv:0711.4866v1 [hep-ph].
37. J. P. Lees et al. (The BABAR Collaboration), Search for Invisible Decays of a Dark Photon Produced in e^+e^- Collisions at BABAR, (2017) arXiv:1702.03327v2 [hep-ex].

38. D. Banerjee et al. (NA64), Search for vector mediator of Dark Matter production in invisible decay mode, (2017), arXiv:1710.00971v2 [hep-ex].
39. E. Izaguirre, G. Krnjaic, P. Schuster and N. Toro, Accelerating the Discovery of Light Dark Matter, (2015), arXiv:1505.00011v1 [hep-ph].
40. B. Batell, M. Pospelov and A. Ritz, Exploring Portals to a Hidden Sector Through Fixed Targets, (2009), arXiv:0906.5614v2 [hep-ph].
41. M. Bonesini et al., On particle production for high energy neutrino beams, (2001), arXiv:hep-ph/0101163v3.
42. S. Teis et al., Pion-Production in Heavy-Ion Collisions at SIS energies, (1996), arXiv:nucl-th/9609009v1.
43. M. Schwartz, Quantum Field Theory and the Standard Model, (Cambridge University Press), (2014).
44. Y. Kahn, G. Krnjaic, J. Thaler and M. Toups, DAEδALUS and Dark Matter Detection, (2014), arXiv:1411.1055v3 [hep-ph].
45. Kevin J. Kelly and Yu-Dai Tsai, Proton Fixed-Target Scintillation Experiment to Search for Minicharged Particles, (2018), arXiv:1812.03998v2 [hep-ph].
46. Johannes Blümlein and Jürgen Brunner, New Exclusion Limits on Dark Gauge Forces from Proton Bremsstrahlung in Beam-Dump Data, (2013), arXiv:1311.3870v1 [hep-ph].
47. D. Gorbunov, A. Makarov, and I. Timiryasov, Decaying light particles in the SHiP experiment:Signal rate estimates for hidden photons, (2015), arXiv:1411.4007v2 [hep-ph].
48. A. Faessler, M. I. Krivoruchenko, and B. V. Martemyanov, Once more on electromagnetic form factors of nucleons in extended vector meson dominance model, (2009), arXiv:0910.5589v1 [hep-ph].
49. P. deNiverville, D. McKeen, and A. Ritz, Signatures of sub-GeV dark matter beams at neutrino experiments, (2012), arXiv:1205.3499v1 [hep-ph].
50. P. M. Nadolsky et al., Implications of CTEQ global analysis for collider observables, (2008), arXiv:0802.0007v3 [hep-ph].
51. P. deNiverville, M. Pospelov, and A. Ritz, Observing a light dark matter beam with neutrino experiments, (2013), arXiv:1107.4580v3 [hep-ph].
52. L.A. Ahrens et al., Measurement of neutrino-proton and antineutrino-proton elastic scattering, Phys. Rev. D35, 785(1987).
53. B. Batell, P. deNiverville, D. McKeen, M. Pospelov, and A. Ritz, Leptophobic Dark Matter at Neutrino Factories, (2014), arXiv:1405.7049v1 [hep-ph].
54. High-Pressure Argon gas TPC Option for the DUNE Near Detector, DUNE HPgTPC WG, Fermi National Accelerator Laboratory, Box 500, Batavia, IL 60510-5011, USA.
55. Garrett BROWN, Sensitivity Study for Low Mass Dark Matter Search at DUNE, (2018).
56. Gert Hütsi et al., WMAP7 and future CMB constraints on annihilating dark matter:implications for GeV-scale WIMPs, (2011), arXiv:1103.2766v3 [astro-ph.CO].
57. Brian Henning and Hitoshi Murayama, Constraints on Light Dark Matter from Big Bang Nucleosynthesis, (2012), arXiv:1205.6479v1 [hep-ph].
58. M. Markevitch et al., Direct constraints on the dark matter self-interaction cross-section from the merging galaxy cluster 1E0657-56, (2004), arXiv:astro-ph/0309303v2.
59. J. Miralda-Escude, A Test of the Collisional Dark Matter Hypothesis from Cluster Lensing, (2001), arXiv:astro-ph/0002050v2.
60. P. Fayet, Invisible Υ decays into Light Dark Matter, (2010), arXiv:0910.2587v2 [hep-ph].
61. R.M. Bionta et al., Observation of a Neutrino Burst in Coincidence with Supernova 1987A in the Large Magellanic Cloud, Phys.Rev.Lett. 58, 1494 (1987);
K. Hirata et al., Observation of a Neutrino Burst from the Supernova SN1987A, (Kamiokande-II), Phys.Rev.Lett. 58, 1490 (1987);
E. Izaguirre, G. Krnjaic, P. Schuster, and N. Toro, Testing GeV-Scale Dark Matter with Fixed-Target Missing Momentum Experiments, (2015), arXiv:1411.1404v3 [hep-ph].
62. G. Angloher et al., (CRESST Collaboration), Results on light dark matter particles with a low-threshold CRESST-IIdetector, Eur. Phys. J. C76, 25 (2016), arXiv:1509.01515 [astro-ph.CO].
63. R. Agnese et al., (SuperCDMS Collaboration), WIMP-Search Results from the Second CDMSlite Run, (2016), arXiv:1509.02448v2 [astro-ph.CO].
64. B. A. Dobrescu and C. Frugiuele, Hidden GeV-scale interactions of quarks, (2014), arXiv:1404.3947v2 [hep-ph].
65. B. Batell, R. Essig, and Z. Surujon, Strong Constraints on Sub-GeV Dark Sectors from SLAC Beam Dump E137, Phys.Rev.Lett. 113, 171802 (2014), arXiv:1406.2698 [hep-ph].
66. M. Pospelov, Secluded U(1) below the weak scale, (2008), arXiv:0811.1030v1 [hep-ph].
67. A. V. Artamonov et al. (E949 Collaboration), Study of the decay $K^+ \to \pi\nu\bar{\nu}$ in the momentum region $140 < P_\pi < 199$ MeV/c, (2009), arXiv:0903.0030v1 [hep-ex].
68. R. Bouchendira et al., New determination of the fine structure constant and test of the quantum electrodynamics, (2010), arXiv:1012.3627v1 [physics.atom-ph].
69. T. Aoyama et al., Tenth-Order QED Contribution to the Electron $g2$ and an Improved Value of the Fine Structure Constant, (2012), arXiv:1205.5368v2 [hep-ph].
70. D. Hanneke, S. F. Hoogerheide, and G. Gabrielse, Cavity Control of a Single-Electron Quantum Cyclotron: Measuring the Electron Magnetic Moment, (2010), arXiv:1009.4831v1 [physics.atom-ph].
71. A.A. Aguilar-Arevalo et al., (The MiniBooNE-DM Collaboration), Dark matter search in nucleon, pion, and electron channels from a proton beam dump with MiniBooNE, (2018), arXiv:1807.06137v2 [hep-ph].
72. A. A. Aguilar-Arevalo et al., (The MiniBooNE-DM Collaboration), A Combined $\nu_\mu \to \nu_e$ & $\bar{\nu}_\mu \to \bar{\nu}_e$ Oscillation Analysis of the MiniBooNE Excesses, (2012), arXiv:1207.4809v2 [hep-ex].

73. Claudia Frugiuele, Probing sub-GeV dark sectors via high energy proton beams at LBNF/DUNE and MiniBooNE, Phys. Rev., D 96, 015029 (2017).
74. Pilar Coloma, Bogdan A. Dobrescu, Claudia Frugiuele and Roni Harnik, Dark matter beams at LBNF, JHEP 04 (2016) 047.
75. R. Essig et al., Constraining Light Dark Matter with Low-Energy e^+e^- Collider , (2015), arXiv:1309.5084v2 [hep-ph].
76. Maíra Dutra et al., MeV Dark Matter Complementarity and the Dark Photon Portal, (2018), arXiv:1801.05447v2 [hep-ph].